ChemPubSoc Europe

DOI: 10.1002/chem.201402146

CHEMISTRY
A European Journal
Full Paper

Sensors

Conformational Changes in Calcium-Sensor Proteins under Molecular Crowding Conditions

Stefan Sulmann,[a] Daniele Dell'Orco,[b] Valerio Marino,[b] Petra Behnen,[c] and Karl-Wilhelm Koch*[a]

Abstract: Fundamental components of signaling pathways are switch modes in key proteins that control start, duration, and ending of diverse signal transduction events. A large group of switch proteins are Ca^{2+} sensors, which undergo conformational changes in response to oscillating intracellular Ca^{2+} concentrations. Here we use dynamic light scattering and a recently developed approach based on surface plasmon resonance to compare the protein dynamics of a diverse set of prototypical Ca^{2+}-binding proteins including calmodulin, troponin C, recoverin, and guanylate cyclase-activating protein. Surface plasmon resonance biosensor technology allows monitoring conformational changes under molecular crowding conditions, yielding for each Ca^{2+}-sensor protein a fingerprint profile that reflects different hydrodynamic properties under changing Ca^{2+} conditions and is extremely sensitive to even fine alterations induced by point mutations. We see, for example, a correlation between surface plasmon resonance, dynamic light scattering, and size-exclusion chromatography data. Thus, changes in protein conformation correlate not only with the hydrodynamic size, but also with a rearrangement of the protein hydration shell and a change of the dielectric constant of water or of the protein–water interface. Our study provides insight into how rather small signaling proteins that have very similar three-dimensional folding patterns differ in their Ca^{2+}-occupied functional state under crowding conditions.

Introduction

Conformational transitions in proteins control the on and off modes of cellular responses in a very precise manner. These conformational changes can be induced, for example, by small organic ligands, protein–protein interactions, or second messengers like Ca^{2+}. The versatile action of Ca^{2+} is based on the operation of hundreds of different Ca^{2+}-sensor proteins that detect changes in intracellular Ca^{2+}, thereby switching into a mode of controlling the function of a target protein.[1] Often, one Ca^{2+}-sensor protein can regulate different targets, among which the most prominent example is probably calmodulin (CaM), a member of the superfamily of EF-hand Ca^{2+}-binding proteins. CaM exhibits a kind of conformational plasticity, meaning it is able to control different target protein function by adopting a fitting conformation for a specific target structure.[2,3] A similar task is probably performed by neuronal Ca^{2+}-sensor (NCS) proteins, a subgroup of the EF-hand superfamily.[4,5] However, despite their rather similar three-dimensional folding, each member of this group may regulate only a few or just one target out of a large diversity of different proteins. For example, rod and cone cells of the vertebrate retina specifically express Ca^{2+}-sensors like recoverin[5] and guanylate cyclase-activating protein 1 (GCAP1),[6–8] of which the latter regulates the activity of sensory membrane guanylate cyclases. Considering the conformational variety of one small Ca^{2+} sensor like CaM[2,3] on the one hand and the similar general folding of NCS proteins[4,5] on the other poses the following questions. Which conformational changes control the on and off states of a particular Ca^{2+} sensor? How do these states differ in proteins of the same subgroup or between mutants and the corresponding wild type?

Fluorescence, circular dichroism, and NMR spectroscopy have been widely employed among other methods to detect conformational changes in proteins. A more recent rather innovative approach was to use the surface plasmon resonance (SPR) phenomenon for the detection of conformational transitions. Two different experimental procedures have mainly been tested so far. Localized SPR (LSPR)[9,10] employs silver or gold nanoparticles coated with the protein under study. Commercial SPR sensors use dextran-coated gold surfaces with covalently and non-covalently attached proteins. By using the latter approach conformational changes have been detected in enzymes, redox proteins, and Ca^{2+}-binding proteins.[11–17] Furthermore, coupled plasmon-waveguide resonance spectroscopy,

[a] S. Sulmann, Prof. Dr. K.-W. Koch
Department of Neurosciences, Biochemistry Group
University of Oldenburg, 26111 Oldenburg (Germany)
E-mail: karl.w.koch@uni-oldenburg.de

[b] Dr. D. Dell'Orco, V. Marino
Department of Life Sciences and Reproduction
Section of Biological Chemistry and Center for BioMedical Computing (CBMC)
University of Verona, Verona (Italy)

[c] Dr. P. Behnen
Department of Biomedical Sciences
University of Modena, Modena (Italy)

Supporting information for this article is available on the WWW under http://dx.doi.org/10.1002/chem.201402146.

a technique related to SPR, has been employed to study conformational changes in G protein-coupled receptors.[18,19] It has been argued that the rather long (ca. 200 nm) decay length of the electromagnetic field in commercially available SPR sensor chips, such as CM5 supplied by Biacore, dramatically reduces the sensitivity to small refractive index changes occurring close to the sensor surface,[10] thus making the much shorter (ca. 5 nm) decay length in LSPR systems more appropriate for detecting a conformational change of an adsorbed protein on its surface. However, SPR responses obtained with proteins immobilized on dextran-coated sensor chips have been clearly correlated with conformational changes using appropriate controls.[11–19] Artefact signals were excluded in a recent study that compares Ca^{2+}-induced conformational changes in the neuronal Ca^{2+}-sensor protein recoverin with a specifically designed recoverin mutant, which does not undergo a Ca^{2+}-triggered conformational change.[16] We noticed that increasing the Ca^{2+} concentration ($[Ca^{2+}]$) into the millimolar range leads to dextran matrix effects on the sensor chip surface independent of the immobilized protein.[16] This study was more recently extended by comparing different Ca^{2+}-sensor proteins under experimental conditions, in which the influence of ionic strength, divalent cations, and different sensor chip surfaces was tested.[17] This SPR-based approach allows us to investigate Ca^{2+}-induced conformational changes in a working range of physiologically relevant free $[Ca^{2+}]$, thereby distinguishing non-specific matrix effects from protein-derived signals in a setting of precisely defined parameters. A further advantage of our method is that it uses a commercial SPR device and a sensor chip, which provides four flow cells to immobilize and investigate up to three proteins and one control surface under identical buffer flow and sample injections.[16,17]

It has been suggested that the solvent around the immobilized protein rearranges during a conformational transition, especially when a significant variation in the hydrophobicity of the solvent-exposed protein surface occurs, thus leading to changes in the dielectric milieu of the whole flow cell of the sensor chip.[11,13,14,16,17]

Based on previous and present observations we sought to discriminate different forms of conformational changes in a set of Ca^{2+}-sensor proteins. For this purpose we determined the Ca^{2+}-dependent changes in the hydrodynamic properties of Ca^{2+}-sensor proteins and compared them with Ca^{2+}-induced SPR responses. Our results confirm that the SPR-based approach is extremely sensitive to even fine alterations induced by mutations in the conformational switch of Ca^{2+}-sensor proteins. The signal depends not only on the change in hydrodynamic protein size upon Ca^{2+}-binding, but likely reflects a different hydration structure, which can be significantly affected in the crowding conditions occurring on the sensor chip.

Results

Ca^{2+}-induced changes in hydrodynamic volume

First, we investigated Ca^{2+}-dependent changes in the hydrodynamic radius of Ca^{2+}-sensor proteins that are known to differ significantly in their conformational transitions. For this purpose we determined the hydrodynamic diameter (d in nm) of several Ca^{2+}-sensor proteins by dynamic light scattering (DLS) in the presence and absence of Ca^{2+}, of which representative results are displayed in Figure 1 for CaM^{S17C}, a mutant of myristoylated recoverin ($mRec^{2-190}$),[20,21] myristoylated GCAP1 (mGCAP1) and troponin C (TnC). These measurements showed a size distribution of light scattering intensity resulting in one peak of high intensity (peak 1) and one of lower intensity (peak 2). However, one exception was observed in the case of TnC, for which the intensity of peak 2 was higher (see also further below). Determination of hydrodynamic diameters revealed for Ca^{2+}-free proteins the following d values (Table 1): 4.97 (CaM^{S17C}), 5.53 ($mRec^{2-190}$), 7.5 (mGCAP1), and 7.88 nm (TnC). Adding saturating Ca^{2+} caused a shift of peak 1 to either higher (CaM^{S17C}, $mRec^{2-190}$) or lower d values (mGCAP1, TnC) indicating a Ca^{2+}-induced change of the hydrodynamic volume. The same set of measurements was performed with wild type myristoylated (m) and nonmyristoylated (nm) recoverin, and with several point mutants of GCAP1 known to cause retinal cone-rod dystrophies[22–24] (Table 1).

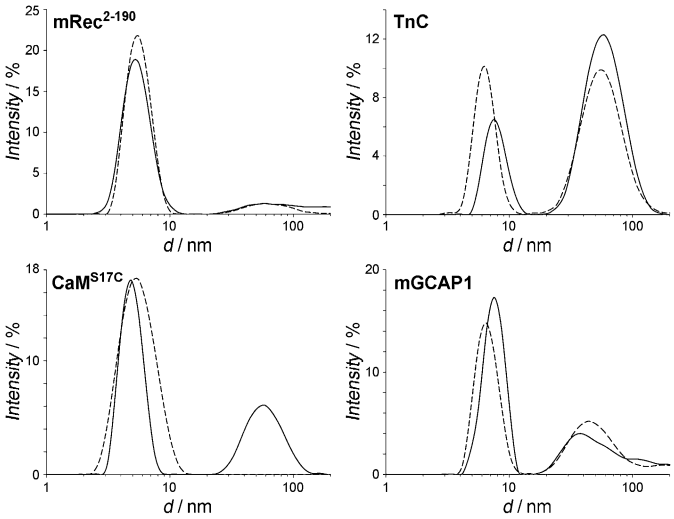

Figure 1. Determination of hydrodynamic diameters of Ca^{2+}-sensor proteins by dynamic light scattering. All measurements were performed at $T = 25\,^{\circ}C$ in 5 mM Tris/HCl pH 7.5, 150 mM KCl buffer. Black solid lines refer to measurements in the presence of saturating EGTA, while dashed lines to saturating Ca^{2+} conditions. Size distributions of: 26 μM $mRec^{2-190}$ in the presence of 240 μM EGTA and 260 μM Ca^{2+} (upper left); 55 μM TnC in the presence of equal amounts (1.5 mM) of saturating EGTA or Ca^{2+} (upper right); 187 μM CaM^{S17C} in the presence of 4 mM EGTA and 5 mM Ca^{2+} (lower left); 60 μM mGCAP1 in the presence of equal amounts (1.5 mM) of saturating EGTA or Ca^{2+}. Data obtained by DLS measurements reporting the intensity of scattered light as % of the total area.

In order to compare the changes in d among all tested Ca^{2+}-sensor proteins in relative and not in absolute terms, we evaluated our data by calculating the relative change $\Delta d/d_{EGTA}$ (Δd is defined as the diameter in the presence of Ca^{2+} minus that in the presence of EGTA ($d_{Ca^{2+}}$-d_{EGTA})). Values for $\Delta d/d_{EGTA}$ of 5.7 and 14.7% were found for recoverin and CaM, respectively

Table 1. Dynamic light scattering measurements of Ca^{2+}-sensor proteins. Determination of the hydrodynamic diameter d from peaks 1 and 2 ($\pm$standard error $= \sigma/N^{1/2}$; N is the number of repetitions; d was determined in the presence or absence of Ca^{2+}. Δd [nm] is the difference $d_{Ca} - d_{EGTA}$ ($\pm$propagation of errors $= (\sigma_1^2 + \sigma_2^2)^{1/2}$. CaM was the S17C-mutant.[17]. Wild type recoverin is abbreviated Rec.

Protein [nm]	d (peak 1) [nm]	d (peak 2) [nm]	N	Δd [nm]	$\Delta d/d_{EGTA}$ [%]
TnC (EGTA)	7.88 ± 0.11	61.78 ± 2.80	21	−1.44 ± 0.30	−18.3
TnC (Ca^{2+})	6.44 ± 0.06	60.22 ± 4.20	21		
CaM (EGTA)	4.97 ± 0.01	62.14 ± 5.50	25	+0.73 ± 0.03	+14.7
CaM (Ca^{2+})	5.70 ± 0.03		25		
$mRec^{2-190}$ (EGTA)	5.53 ± 0.05		23	+0.13 ± 0.06	+2.3
$mRec^{2-190}$ (Ca^{2+})	5.66 ± 0.02		26		
mRec (EGTA)	5.22 ± 0.02	79.91 ± 11.10	20	+0.30 ± 0.03	+5.7
mRec (Ca^{2+})	5.52 ± 0.02	78.60 ± 5.20	19		
nmRec (EGTA)	5.57 ± 0.06	37.43 ± 1.57	12	−0.23 ± 0.10	−4
nmRec (Ca^{2+})	5.34 ± 0.08	36.18 ± 1.50	13		
mGCAP1 (EGTA)	7.5 ± 0.2		20	−0.8 ± 0.2	−10.3
mGCAP1 (Ca^{2+})	6.69 ± 0.04		26		
D100E (EGTA)	7.82 ± 0.12		21	−1.08 ± 0.14	−13.8
D100E (Ca^{2+})	6.74 ± 0.07	29.48 ± 3.34	18		
L151F (EGTA)	7.50 ± 0.11	26.82 ± 4.60	27	−0.42 ± 0.19	−5.6
L151F (Ca^{2+})	7.08 ± 0.15	26.65 ± 6.50	20		
E89K (EGTA)	8.30 ± 0.09	44 ± 17	21	−0.6 ± 0.1	−7.2
E89K (Ca^{2+})	7.70 ± 0.09	40.40 ± 13.38	25		
nmGCAP1 (EGTA)	6.25 ± 0.05		23	+0.51 ± 0.09	+8.2
nmGCAP1 (Ca^{2+})	6.76 ± 0.07		26		

(Table 1). Deletion of twelve amino acids at the C-terminus of recoverin in the mutant Rec^{2-190} diminished the Ca^{2+}-dependent change in d yielding a $\Delta d/d_{EGTA} = 2.3\%$, which is consistent with previous reports identifying this region as Ca^{2+}-sensitive control module.[20,21] Changes in TnC were also large, but with an inverted sign of $\Delta d/d_{EGTA}$ (−18.3%).

GCAP1 is an NCS protein like recoverin, but does not show a large rearrangement of its myristoyl group.[25] Interestingly, it also displayed a pronounced change in d ($\Delta d/d_{EGTA} = -10.3\%$). Wild type (WT) GCAP1 was further compared with several of its single-point mutants known to cause retinal cone-rod dystrophies.[22–24] Ca^{2+}-saturated GCAP1 mutants had a d value of around 7 nm, which is not much different to that of WT. However, the relative changes $\Delta d/d_{EGTA}$ showed a larger variation yielding −5.6% for L151F, −7.2% for E89 K and −13.8% for D100E (Table 1).

Intensity peaks corresponding to higher order oligomers were detected for each protein, and they were particular apparent for TnC. Their effective weight on the photon correlation signal is, however, modest due to the $1/d^6$ scaling of scattered light intensity. Monitoring number and volume distributions of the same molecular species in fact confirmed that monomers were the most populated species in each case.

DLS measurements confirmed that all tested Ca^{2+}-sensor proteins undergo significant Ca^{2+}-induced changes in their hydrodynamic volume. However, the relative changes expressed in $\Delta d/d_{EGTA}$ are rather different among the proteins and even became visible among myristoylated and nonmyristoylated protein forms. Ca^{2+}-induced changes in WT recoverin and WT GCAP1 led to significant Δd and $\Delta d/d_{EGTA}$ values, but sign inversion occurred when a myristoyl group was posttranslational attached to the protein (Table 1).

Detection of Ca^{2+}-switch modes by an SPR biosensor

An alternative approach to detect differences in Ca^{2+}-induced protein dynamics had previously been reported for recoverin, CaM, GCAP1, and GCAP2 using SPR.[16,17] Therefore, we hypothesized that the diverse switch modes of Ca^{2+}-sensor proteins, which we observed by dynamic light scattering, can also be detected using the SPR approach and we included in the present study Ca^{2+} titrations with TnC, $mRec^{2-190}$ and the GCAP1 mutants E89K, D100E, L151F, and G159V (Figure 2). TnC on the chip surface reacted to increasing [Ca^{2+}] with responses of increasing amplitudes reaching saturation at >30 μM Ca^{2+} (Figure 2, upper panel). A similar Ca^{2+} sensitivity was observed with the recoverin mutant Rec^{2-190} (Figure 2, lower panel), which was almost identical to previously determined values of the wild type (Table 2). However, the maximal amplitudes that were reached at the end of the titrations were

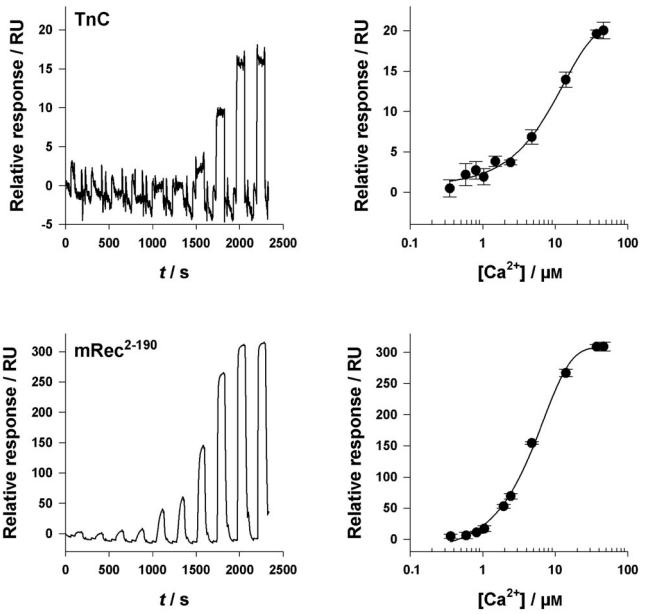

Figure 2. SPR responses of Ca^{2+}-sensor proteins at increasing free [Ca^{2+}]. Examples of sensorgrams obtained upon Ca^{2+} titrations (left panel). The response amplitude at the end of each Ca^{2+} injection is plotted as a function of Ca^{2+} (right panel; the error bars represent the SD). Sensorgrams were obtained for TnC and the myristoylated recoverin mutant Rec^{2-190}. Data fitting by a Hill sigmoidal curve resulted in $K_{1/2}^{SPR} = 11.5 \pm 0.3$ μM for TnC ($n = 5$) and a $K_{1/2}^{SPR} = 4.90 \pm 0.02$ μM ($n = 8$) for Rec^{2-190}.

Table 2. SPR-based detection of conformational changes expressed in half-maximal values of response amplitudes and normalized RU_{max} values. CaM was the S17C-mutant.[17]

Protein	Divalent cations	$K_{1/2}^{SPR}$ [μM]	Normalized RU_{max}
TnC	Ca^{2+}	11.5 ± 0.3	10.2 ± 0.5
$mRec^{2-190}$	Ca^{2+}	4.90 ± 0.02	39.9 ± 0.9
mGCAP1[a]	Ca^{2+}	19.7 ± 0.8	2.3 ± 0.1
	$Ca^{2+} + Mg^{2+}$	25.4 ± 1.2	1.0 ± 0.1
mE89K	Ca^{2+}	30.8 ± 1.4	1.8 ± 0.1
	$Ca^{2+} + Mg^{2+}$	59.9 ± 0.7	1.5 ± 0.1
mD100E	Ca^{2+}	20.9 ± 0.3	2.6 ± 0.1
	$Ca^{2+} + Mg^{2+}$	45.8 ± 0.7	1.5 ± 0.1
mL151F	Ca^{2+}	31.6 ± 0.6	1.9 ± 0.1
	$Ca^{2+} + Mg^{2+}$	52.4 ± 1.4	1.1 ± 0.1
mG159V	Ca^{2+}	24.0 ± 1.1	2.0 ± 0.1
	$Ca^{2+} + Mg^{2+}$	79.4 ± 2.3	1.1 ± 0.1
CaM[a]	Ca^{2+}	5.70 ± 0.03	11.7 ± 0.1
	$Ca^{2+} + Mg^{2+}$	17.2 ± 0.4	6.6 ± 0.1
mGCAP2[a]	Ca^{2+}	24.9 ± 0.2	3.6 ± 0.3
	$Ca^{2+} + Mg^{2+}$	37.7 ± 0.5	2.0 ± 0.1
mRec[a]	Ca^{2+}	5.0 ± 0.2	36.3 ± 0.3
	$Ca^{2+} + Mg^{2+}$	5.2 ± 0.1	19.5 ± 0.1

[a] See reference [17].

dramatically different between TnC and Rec^{2-190} (Table 2). This was partly due to differences in immobilization density, which was in all tests much lower for TnC than for all recoverin forms (see the Experimental Section and below). Additionally, differences in the structure and dynamics of the protein hydration shell contribute to the observed effects (see also the Discussion section). Mutants of GCAP1 also showed a characteristic response pattern (Figure 3) allowing the determination of the $[Ca^{2+}]$ at which the increase in response amplitude is half maximal ($K_{1/2}^{SPR}$ in Table 2). The $K_{1/2}^{SPR}$ of the GCAP1 mutants was shifted to higher $[Ca^{2+}]$, indicating a decrease in Ca^{2+}-binding affinity, which is in agreement with previous results that these cone-rod dystrophy related mutations cause a change in Ca^{2+} sensitivity.[23,24] The experiments were also performed in the presence of physiological levels of free magnesium. The presence of 1 mM Mg^{2+} during the Ca^{2+}-titrations had mainly two effects; it decreased the response amplitudes and increased the $K_{1/2}^{SPR}$ of both WT and mutant GCAP1 (Figure 3 and Table 2). Thus, the Ca^{2+} titrations displayed two main features that were characteristic for each protein: the $K_{1/2}^{SPR}$ and different amplitudes that were reached at saturating $[Ca^{2+}]$ (Figures 2 and 3).

The response amplitudes of the titration series at saturating Ca^{2+} were normalized to the amount of immobilized protein and were defined as normalized RU_{max} (Table 2). It became clear that response amplitudes were highly dependent on the type of protein as well as on the immobilization technique. However, a different chemistry of coupling does not significantly affect the $K_{1/2}^{SPR}$, instead it results in important variation of response amplitudes reached at the end of each analyte injection.[16] Therefore we compared quantitatively the results from the three techniques employed in this work on a series of GCAP1 mutants, which were all immobilized by means of amine coupling at similar amounts on the sensor chip surface. We point out that detecting subtle variations in the conformational properties of proteins differing from one another only by a single-point mutation represents a proof of the sensitivity of the approach. Figure 4 reports the results of quantitative comparisons. The SPR signal clearly correlates with the change

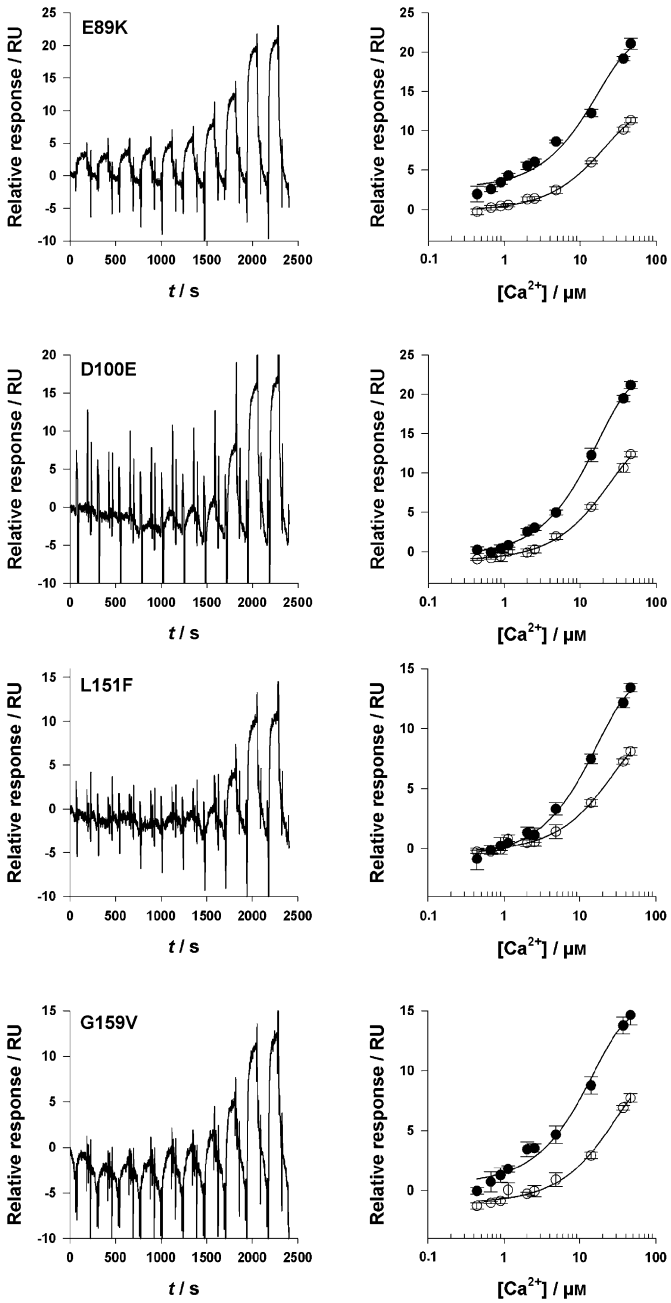

Figure 3. Sensorgrams obtained for myristoylated GCAP1 mutants E89K, D100E, L151F and G159V. Sensorgrams are on the left panel, evaluation of data without Mg^{2+} (●) and in the presence of 1 mM free Mg^{2+} (○) is shown on the right panel. Data fitting by a Hill sigmoidal curve resulted in the following values of $K_{1/2}^{SPR}$ (in brackets): E89K (30.8 ± 1.4 μM; $n = 4$); D100E (20.9 ± 0.3 μM, $n = 3$), L151F (31.6 ± 0.6 μM, $n = 4$), G159V (24. ± 1.1 μM, $n = 3$). Values of $K_{1/2}^{SPR}$ in the presence of 1 mM Mg^{2+} were: E89K (59.9 ± 0.7 μM; $n = 6$); D100E (45.8 ± 0.7 μM, $n = 5$), L151F (52.4 ± 1.4 μM, $n = 6$), G159V (79.4 ± 2.3 μM, $n = 4$). Error bars represent the standard deviation.

in hydrodynamic radius as detected both by size exclusion chromatography (SEC) ($R^2 = 0.83$) and DLS ($R^2 = 0.88$), thus confirming that the signal originates from changes in hydrodynamic properties of the protein upon Ca^{2+} binding.

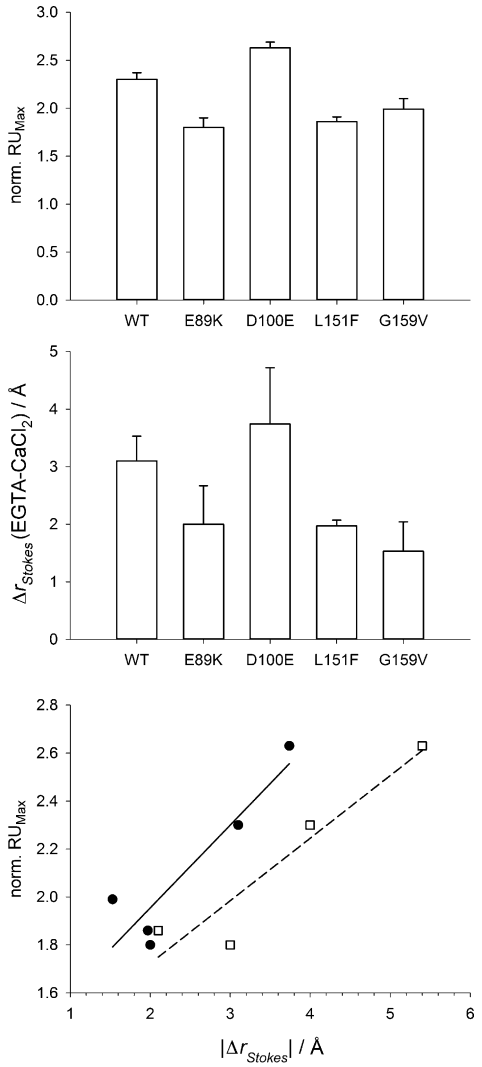

Figure 4. Comparison of normalized RU_{max} values and differences in Stokes radii ($|\Delta r_{Stokes}| = |r_{Stokes}^{EGTA} - r_{Stokes}^{Ca^{2+}}|$) for the series of mGCAP1 variants. The upper panel shows the normalized values of RU_{max} obtained from Ca^{2+} titration series as seen in Figure 2 for myristoylated GCAP1 WT and the mutants E89K, D100E, L151F, and G159V. Differences in Stokes radii were obtained both from analytical size exclusion chromatography (mid panel) and dynamic light scattering (see Table 1), and the absolute value of the variation linearly correlates with RU_{max} in both cases (lower panel: ●:SEC data set ($R^2 = 0.83$); □: DLS data set ($R^2 = 0.88$)).

Discussion

Ca^{2+}-sensor proteins like recoverin and CaM undergo extensive changes in their three-dimensional structure upon Ca^{2+} binding[2,3,5] and thereby switch between on and off modes. Multifunctional Ca^{2+} sensors like CaM, however, can operate in more complex ways by, for example, controlling target function in Ca^{2+}-bound and Ca^{2+}-free states.[1–3] In the present work, we investigated how protein parameters like size and hydrodynamic volume change, when a Ca^{2+} sensor is switching between Ca^{2+}-bound and Ca^{2+}-free states. Large structural changes in recoverin and CaM were mirrored in significant changes of their hydrodynamic diameters (Table 1). Further, we employed classical techniques like DLS and SEC, which provided us with a data set that for each protein gave a fingerprint profile reflecting different hydrodynamic properties. For example, CaM and TnC showed among all tested Ca^{2+}-sensor proteins the largest differences in size (Ca^{2+}-free versus Ca^{2+}-bound), and SPR confirmed these important variations. However, a clear mismatch was observed for recoverin and its truncated mutant Rec^{2-190}, for which relative changes in size determined by DLS differed significantly from each other, and were less prominent compared to CaM and TnC, (Table 1), at odds with determinations by SPR (Figure 2, Table 2). On the other hand, when the same set of GCAP1 mutant was similarly compared, DLS, SEC, and SPR showed consistent results (Figure 4). Where does this discrepancy originate from? We previously analyzed[16] the available structural data on recoverin and postulated that the significant increase in hydrophobicity upon Ca^{2+} binding would reflect on the structure of the hydration shell, and consequently on the refractive index of the protein–water dielectric milieu, which is the physical signal detected by SPR instruments. It is in fact known that, owing to the lack of hydrogen bonds, water molecules near hydrophobic surfaces behave different from bulk water.[26] The different properties of hydration water in terms of local density reflect in a different dielectric constant and eventually refractive index, which is its square root. This is, however, true for both proteins in solution, like in SEC and DLS experiments, and those immobilized on the SPR sensor chip. What is significantly different in the two situations is the molecular crowding, which is definitely higher in the SPR conditions and might affect differently the structure and dynamics of the hydration shell.[26]

Physiological protein solutions in a cellular environment are highly concentrated (up to 400 g L^{-1}) filling 5–40% of the total cell volume.[27] As we have pointed out in a recent publication the SPR approach for detecting conformational changes relies on a high amount of immobilized protein in a dextran-like mesh.[17] Therefore, it differs from the "canonical" use of the SPR technology (particularly the Biacore system), in which low immobilization levels on the sensor chip surface should be achieved in order to obtain reliable kinetic constants.[28] However, it was not the aim of the present study to extract kinetic constants from the sensorgrams. Instead we have a high density of proteins covalently attached to a 100 nm dextran layer mimicking crowding effects, for which inert synthetic polymers including dextran are often used.[29,30]

The Ca^{2+}-dependent changes of CaM in the presence of crowding reagents differ significantly from those of the diluted protein solution.[31] Our results here indicate that this conclusion might be true for a variety of different sensor proteins pointing to a more general principle. However, the parameter $K_{1/2}^{SPR}$ that we determined here is different from apparent K_D values for direct Ca^{2+} binding to recoverin[16,20,21] and GCAP1 forms[24,32] or values that describe the [Ca^{2+}], at which a biologi-

cal regulatory effect is halfmaximal (IC_{50}, EC_{50}).[4–8,20–23,25] In our previous work[17] we related apparent K_D values of Ca^{2+} binding to $K_{1/2}^{SPR}$ by the equation $K_D^{app} = K_{cc} \times K_{1/2}^{SPR}$, in which K_{cc} is a unitless quantity defined as conformational change contribution. Thus, the empirical parameter $K_{1/2}^{SPR}$ is a useful tool to describe a concerted binding-conformational switch, either among different, but related, proteins or under conditions that influence conformational transitions.[17]

Then, how can SPR signals of increasing amplitudes at increasing [Ca^{2+}] be interpreted? SPR signals originate from changes in the refractive index close to the sensor surface and the refractive index equals the square root of the dielectric constant of the medium and of the soluble compounds. Although the dextran–protein compartment on the surface of the sensor chip is in an aqueous environment the relative dielectric constant of water in a crowded protein environment is lower than $\varepsilon = 80$, the value in bulk solution. In our SPR experiments the volume fraction of the immobilized protein is around 0.2 (Supporting Information) and under these conditions the ε of water decreases to about 60.[26] The maximal amplitudes that we observed in different Ca^{2+}-sensor proteins are between 10 and 300 RU, which correspond to a relative change[33] in bulk refractive index of 10^{-5} to 3×10^{-4}. The relative change $\Delta\varepsilon_r$ in dielectric constant of the aqueous protein–dextran compartment corresponds to 3.2×10^{-3} and 1.7×10^{-2}, respectively. Thus, the Ca^{2+}-induced conformational changes for proteins like recoverin as detected by SPR are accompanied by an approximately fivefold higher change in dielectric constant compared to GCAP1 variants, higher than the relative change attributed to water when passing from bulk to a highly crowded environment. We therefore conclude that the changes in protein conformation correlate with a rearrangement of both the hydration shell and the hydrodynamic protein properties (see above). We further conclude that the positive SPR amplitudes during a Ca^{2+} titration originate from an increase of the dielectric constant of water or of the protein–water interface. Thus, it would reflect a less "crowded" state in the dextran matrix, when Ca^{2+} is bound to Ca^{2+}-sensor proteins like recoverin, GCAPs, and CaM. If this hypothesis is true, one should find conditions under which Ca^{2+} titrations result in negative SPR amplitudes. In fact, we observed in a previous paper[17] that the nonmyristoylated forms of recoverin and GCAP1 exhibited negative amplitudes indicating a kind of reverse process with a lowering of ε (water). This observation would also be consistent with our dynamic light scattering measurements, during which changes in hydrodynamic diameter and $\Delta d/d_{EGTA}$ occurred with sign inversion. Indeed, when taken as absolute values, changes in hydrodynamic radii as detected by SEC and DLS significantly correlate with changes in SPR signals (Figure 4).

Conclusion

We determined physicochemical properties for a set of Ca^{2+}-sensor proteins that regulate the activity of various target proteins like kinases, cyclases, and ion channels. They operate by performing Ca^{2+}-induced switches between on and off states that are triggered by incremental changes of Ca^{2+}, which are significant for cellular processes. We here show that these Ca^{2+} sensors exhibit different responses to changing [Ca^{2+}] in combination with the surrounding water shell. In particular, we were able to correlate data from the SPR biosensor approach, dynamic light scattering, and size exclusion chromatography experiments. Thereby, we obtained characteristic fingerprint profiles relevant for the proteins under conditions of molecular crowding.

Experimental Section

Preparation of protein samples, buffers and calcium stocks

Wild type and mutant forms of recoverin and GCAP1 were heterologously expressed in *E. coli* and purified to homogeneity as described previously.[20–24] The recoverin mutant $mRec^{2-190}$ was a variant of myristoylated recoverin that lacks 12 residues at the C-terminus.[20,21] Preparation and use of CaM^{S17C} in SPR experiments containing a Cys at position 17 have been described previously.[17] Samples used in this work were a kind gift of Prof. Sara Linse (University of Lund, Sweden). Troponin C (TnC) was commercially obtained from Apollo Scientific Ltd., Stockport, UK.

For SPR experiments, we used the SPR running buffer consisting of 5 mM Tris/HCl pH 7.5, 150 mM KCl. For removing Ca^{2+} contaminants the buffer was applied on a Chelex 100 resin column (Biorad) with a flow rate of 3 mL min^{-1}. Treatment of the Chelex resin before use was exactly as described previously.[16,17] The remaining concentration of Ca^{2+} in the buffer after decalcification was measured by withdrawing a small volume and by performing a BAPTA absorption assay as described.[17] It was found to range between 0.11 and 0.20 μM. For the Ca^{2+} titration experiments we used $CaCl_2$ of the highest grade available, dissolved it in the decalcified buffer to a final concentration of 46 mM. This Ca^{2+} stock solution was used to obtain Ca^{2+} stocks of lower concentration by subsequent dilutions to the following final concentrations used in SPR experiments (injections in Figure 2): 0.4, 0.7, 0.9, 1.1, 1.6, 2.5, 4.8, 14, 37, 46.2 μM. All buffers were filtered (0.22 μm) and degassed for at least 1 h before use. For SPR runs Tween20 was added at a final concentration of 0.005% (v/v).

Dynamic light scattering

DLS measurements were performed with a Zetasizer Nano-S (Malvern Instruments) using a polystyrene, low-volume, disposable, sizing cuvette (ZEN0112). Viscosity and refractive index were set to 0.8872 cP and 1.330 (default values for water), temperature was set to 25 °C with 2 min equilibration time. The measurement angle was 173° backscatter and the analysis model was set to multiple narrow modes. For each measurement a minimum of 12 determinations were performed, each consisting of 13–15 repetitions. Buffers (5 mM Tris-HCl, 150 mM KCl, pH 7.5, adjusted with saturating levels of $CaCl_2$ or EGTA), were filtered through a Jet Biofilm 0.22 μm membrane, while protein-only solutions were filtered through an Anotop 10 filter (Whatman, 0.02 μm).

SPR experiments and data analysis

A Biacore2000 surface plasmon resonance instrument (GE Healthcare) was employed for detecting conformational changes in Ca^{2+}-sensor proteins upon injections of Ca^{2+}. Proteins were immobilized at high surface densities on commercial CM5 sensor chips (GE

Healthcare, Uppsala, Sweden). Changes in resonance units (RU) after immobilization are at 2000–9000 RU (1000 RU correspond to 1 ng protein per mm^2).[33] Typical immobilization densities were 2 $ng \times mm^{-2}$ (TnC), 7 $ng \times mm^{-2}$ (GCAP1 forms), 8 $ng \times mm^{-2}$ (CaM^{S17C}) and 9 $ng \times mm^{-2}$ (recoverin forms). CaM^{S17C} and recoverin forms were immobilized by means of thiol coupling, GCAP1 forms by means of amine coupling. Details about general performance of SPR experiments, of Ca^{2+} titrations, and data evaluation have been described,[16,17] but a brief summary is given in the following. Ca^{2+} solutions of increasing free [Ca^{2+}] were injected for 2 min into SPR running buffer (see above). Control injections over a blank surface were done in parallel and were subtracted from sensorgrams obtained with protein coated surfaces. The response amplitude of each Ca^{2+} injection was determined by measuring the difference between RU at start and end of the corresponding Ca^{2+} injection yielding Ca^{2+} titration series. Plotting the response amplitude as a function of Ca^{2+} yields the [Ca^{2+}], at which the response amplitude is half maximal ($K_{1/2}^{SPR}$) as described in detail before.[17] Maximal amplitudes of Ca^{2+} titration series were divided by the amount of immobilized protein yielding normalized RU_{max} values.

Analytical size exclusion chromatography

Ca^{2+}-sensor proteins were analyzed by size exclusion chromatography using a Bio-Sept SEC2000 column (250×4 mm, Phenomenex, Aschaffenburg, Germany). Standard proteins for calibration were bovine serum albumin (66 kDa, Stokes radius 35.5 Å), ovalbumin (43 kDa, Stokes radius 30.5 Å), carboanhydrase (30 kDa, Stokes radius 23.6 Å), myoglobin (17.8 kDa, Stokes radius 20.2 Å), and ribonuclease (13.7 kDa, Stokes radius 16.4 Å). Buffer used in chromatography was the SPR running buffer (s. above) with either 1 mM $CaCl_2$ or 1 mM EGTA added. The protein (50 to 150 μg) was applied on the column and the elution profile was recorded at 280 nm. Elution volumes V_e of Ca^{2+}-sensor proteins were determined at high and low [Ca^{2+}] and the distribution coefficient K_{AV} was calculated according to $K_{AV}=(V_e-V_0)/(V_t-V_0)$, in which V_t is the total column volume and V_0 is the void volume. Stokes radii were determined from a calibration plot of log Stokes radius versus K_{AV} from 4–9 different chromatography runs.

Acknowledgements

This work was supported by the Deutsche Forschungsgemeinschaft (DFG) to K.-W.K. (KO948/10–1) and by funds from the Italian Ministry for Research and Education via departmental funds to D.D.O..

Keywords: calcium sensor · conformational change · protein crowding · protein folding · surface plasmon resonance

[1] M. J. Berridge, M. D. Bootman, H. L. Roderick, *Nat. Rev. Mol. Cell Biol.* **2003**, *4*, 517–529.
[2] S. W. Vetter, E. Leclerc, *Eur. J. Biochem.* **2003**, *270*, 404–414.
[3] M. Ikura, J. B. Ames, *Proc. Natl. Acad. Sci. USA* **2006**, *103*, 1159–1164.
[4] R. D. Burgoyne, *Nat. Rev. Neurosci.* **2007**, *8*, 182–193.
[5] P. P. Philippov, K.-W. Koch, *Neuronal Calcium Sensor Proteins*, Nova Publishers, Hauppauge, NY, **2006**.
[6] K. Palczewski, I. Subbaraya, W. A. Gorczyca, B. S. Helekar, C. C. Ruiz, H. Ohguro, J. Huang, X. Zhao, J. W. Crabb, R. S. Johnson, W. Baehr, *Neuron* **1994**, *13*, 395–404.
[7] S. Frins, W. Bönigk, F. Müller, R. Kellner, K.-W. Koch, *J. Biol. Chem.* **1996**, *271*, 8022–8027.
[8] I. V. Peshenko, A. M. Dizhoor, *J. Biol. Chem.* **2006**, *281*, 23830–23841.
[9] W. Paige Hall, J. N. Anker, Y. Lin, J. Modica, M. Mrksich, R. P. Van Duyne, *J. Am. Chem. Soc.* **2008**, *130*, 5836–5837.
[10] W. Paige Hall, J. Modica, J. N. Anker, Y. Lin, M. Mrksich, R. P. Van Duyne, *Nano Lett.* **2011**, *11*, 1098–1105.
[11] H. Sota, Y. Hasegawa, *Anal. Chem.* **1998**, *70*, 2019–2024.
[12] S. Boussaad, J. Pean, N. J. Tao, *Anal. Chem.* **2000**, *72*, 222–226.
[13] J. E. Gestwicki, H. V. Hsieh, J. B. Pitner, *Anal. Chem.* **2001**, *73*, 5732–5737.
[14] T. Mannen, S. Yamaguchi, J. Honda, S. Sugimoto, A. Kitayama, T. Nagamune, *Anal. Biochem.* **2001**, *293*, 185–193.
[15] T. Christopeit, T. Gossas, U. H. Danielson, *Anal. Biochem.* **2009**, *391*, 39–44.
[16] D. Dell'Orco, M. Müller, K.-W. Koch, *Chem. Commun.* **2010**, *46*, 7316–7318.
[17] D. Dell'Orco, S. Sulmann, S. Linse, K.-W. Koch, *Anal. Chem.* **2012**, *84*, 2982–2989.
[18] Z. Salamon, Y. Wang, M. F. Brown, H. A. MacLeod, G. Tollin, *Biochemistry* **1994**, *33*, 13706–13711.
[19] Z. Salamon, S. Cowell, E. Varga, H. I. Yamagura, V. J. Hruby, G. Tollin, *Biophys. J.* **2000**, *79*, 2463–2474.
[20] O. Weiergräber, I. I. Senin, E. Y. Zernii, V. A. Churumova, N. A. Kovaleva, A. A. Nazipova, S. E. Permyakov, E. A. Permyakov, P. P. Philippov, J. Granzin, K.-W. Koch, *J. Biol. Chem.* **2006**, *281*, 37594–37602.
[21] E. Zernii, K. Komolov, S. Permyakov, T. Kolpakova, D. Dell'Orco, A. Poetzsch, E. Knyazeva, I. Grigoriev, E. Permyakov, I. Senin, P. P. Philippov, K.-W. Koch, *Biochem. J.* **2011**, *435*, 441–450.
[22] V. B. D. Kitiratschky, P. Behnen, U. Kellner, J. R. Heckenlively, E. Zrenner, H. Jägle, S. Kohl, B. Wissinger, K.-W. Koch, *Hum. Mutat.* **2009**, *30*, E782–796.
[23] D. Dell'Orco, P. Behnen, S. Linse, K.-W. Koch, *Cell. Mol. Life Sci.* **2010**, *67*, 973–984.
[24] L. Jiang, T. Z. Li, S. E. Boye, W. W. Hauswirth, J. M. Frederick, W. Baehr, *PLoS One* **2013**, *8*, e57676.
[25] R. Stephen, G. Bereta, M. Golczak, K. Palczewski, M. C. Sousa, *Structure* **2007**, *15*, 1392–1402.
[26] R. Harada, Y. Sugita, M. Feig, *J. Am. Chem. Soc.* **2012**, *134*, 4842–4849.
[27] R. J. Ellis, A. P. Minton, *Nature* **2003**, *425*, 27.
[28] D. Myszka, *J. Mol. Recognit.* **1999**, *12*, 279–284.
[29] S. B. Zimmerman, A. P. Minton, *Annu. Rev. Biophys. Biomol. Struct.* **1993**, *22*, 27–65.
[30] D. J. Winzor, P. R. Wills, *Biophys. Chem.* **2006**, *119*, 186–195.
[31] D. Homouz, H. Sanabria, M. N. Waxham, M. S. Cheung, *J. Mol. Biol.* **2009**, *391*, 933–943.
[32] S. Lim, I. Peshenko, A. Dizhoor, J. B. Ames, *Biochemistry* **2009**, *48*, 850–862.
[33] *Biacore 2000 Instrument Handbook*, Biacore AB **2001**.

Received: February 12, 2014
Published online on ■■ ■■, 0000

FULL PAPER

Sensors

*S. Sulmann, D. Dell'Orco, V. Marino, P. Behnen, K.-W. Koch**

■■ – ■■

Conformational Changes in Calcium-Sensor Proteins under Molecular Crowding Conditions

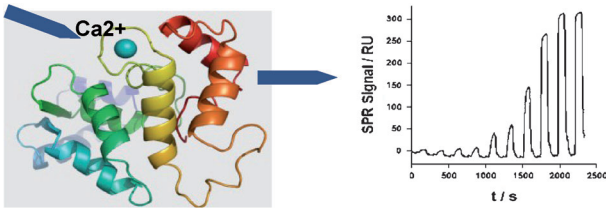

Fingerprint profiles of Ca^{2+} sensors: Ca^{2+}-sensor proteins respond to incremental changes of intracellular Ca^{2+} and regulate diverse cellular responses. These fine-tuned responses are based on specific protein folding patterns, which correlate to changes of the hydrodynamic protein shell and can be monitored by a recently developed method based on surface plasmon resonance spectroscopy (see figure).